

## A DFT study on the electronic structure of tungsten trioxide polymorphs

Masoud MANSOURI, Tahereh MAHMOODI\*

Department of Physics, Faculty of Sciences, Mashhad Branch, Islamic Azad University, Mashhad, Iran

Received: 01.01.2017

Accepted/Published Online: 20.02.2017

Final Version: 13.06.2017

**Abstract:** Tungsten trioxide ( $WO_3$ ) is an intermediate product in the recovery of tungsten from its minerals. Recently, it has attracted increasing attention due to its exclusive structural properties and its high potential in electronic applications. The crystal lattice of tungsten trioxide is highly dependent on temperature. In this paper we investigated the equilibrium structure of tungsten trioxide in four crystal systems, i.e. monoclinic system, tetragonal system, orthorhombic system, and cubic system. We did our first principle calculations using a pseudopotential model based on the spin dependent density functional theory and implementing generalized gradient approximation for exchange correlation energy. In each case, we calculated total energy, Fermi energy, band structure, and density of states and then we made comparisons. The results show that  $WO_3$  is a semiconductor in all four crystal structures with zero total magnetization. Moreover, tungsten trioxide has a direct band gap in the range of visible wavelength that improves its optical applications potentially.

**Key words:** Tungsten trioxide, polymorph, band gap, DOS

### 1. Introduction

Tungsten trioxide ( $WO_3$ ) is a chemical compound that is obtained as an intermediate product in the recovery of tungsten from its minerals. In recent decades, it has been observed that tungsten trioxide has many exclusive electronic properties that can be used in a wide range of applications such as electrochromic devices, smart windows, gas sensors, and solar cells [1–5]. Furthermore, low cost, high chemical activity, nontoxicity, and simple structure are just a few of the main ideal intrinsic properties. Experimental studies show that the crystal lattice of  $WO_3$  is highly temperature dependent. Based on several experimental methods like photoacoustic spectroscopy (PAS) or X-ray absorption near edge structure (XANES), it is demonstrated that pure  $WO_3$  is a semiconductor with a relatively wide band gap range from 2.5 to 3.0 eV [6–8]. Although the stable phase of pure  $WO_3$  at 17–330 °C is monoclinic with the P21/n space group [9], any change in temperature may induce structural distortions and thereby a phase transfer occurs. Indeed, tungsten trioxide has an orthorhombic lattice at 330–740 °C and a tetragonal structure above 740 °C. Furthermore, it can be crystalized in a  $ReO_3$  cubic system without a central atom. It is obvious that the electronic structure of  $WO_3$  is affected by its crystal symmetry. In order to investigate this issue, we performed a comparative study of tungsten trioxide in its three Bravais lattices using first principle calculations.

In the present study the band structure and density of states of  $WO_3$  with the orbital-resolved contributions from tungsten and oxygen atoms were theoretically obtained through DFT calculations in the four mentioned polymorphs.

\*Correspondence: tmahmoodi@mshdiau.ac.ir

## 2. Computational details

We have solved the self-consistent equations of Kohn–Sham using the Quantum-ESPRESSO package, which is based on density functional theory (DFT), and implementing a pseudopotential method [10,11]. Generalized gradient approximation (GGA) and the Perdew–Burke–Ernzerhof (PBE) functional were used for electron exchange-correlation energy [12,13]. In all cases, the converged value for kinetic energy cut-off of 60 Ry was used to guarantee the accuracy up to 0.001 Ry. In addition, an appropriate Monkhorst–Pack grid [14] with the gamma-point included was applied for the integration of the Brillouin zone in each kind of lattice calculation. Moreover, to consider the possibility of a metallic phase, a gaussian broadening with a width of 0.01 eV for smearing was chosen.

In this calculation, four polymorphs of monoclinic, orthorhombic, cubic, and tetragonal systems of tungsten trioxides were studied extensively. All of the structures were fully relaxed and the optimized geometry with minimum total energy and interatomic forces was obtained. To explore the magnetic properties of the polymorphs, a spin polarized approach was employed and band structure, density of states (DOS), and projected density of states (PDOS) were calculated and analyzed in each case.

## 3. Results and discussion

As indicated previously, we studied  $WO_3$  in four crystal structures of orthorhombic with Pnma space group, monoclinic with P21/n space group, tetragonal with P4/nmm space group, and cubic with Pm3m space group. Regarding that a tungsten atom has six oxygen atoms as its nearest neighbors, in all structures, a super cell with eight atoms containing 2 oxygen atoms and 6 tungsten atoms was used, except for the monoclinic lattice, which we treated as a bigger supercell with 32 atoms in it (8 tungsten and 24 oxygen), to improve the results. After the relaxation calculation and obtaining the optimized parameters, to investigate the effect of lattice on electronic properties of  $WO_3$ , band structures (BS), DOS, and PDOS were obtained and analyzed extensively.

Figure 1 shows the optimized supercells in each case. Lattice parameters,  $E_{HOMO}$ ,  $E_{LUMO}$ , and energy gap are also indicated in the Table.  $E_{HOMO}$  is the highest occupied orbital energy and  $E_{LUMO}$  is the lowest unoccupied orbital energy. According to the DFT calculation, the absolute value of  $E_{HOMO}$  is equal to the minimum of the ionization energy.

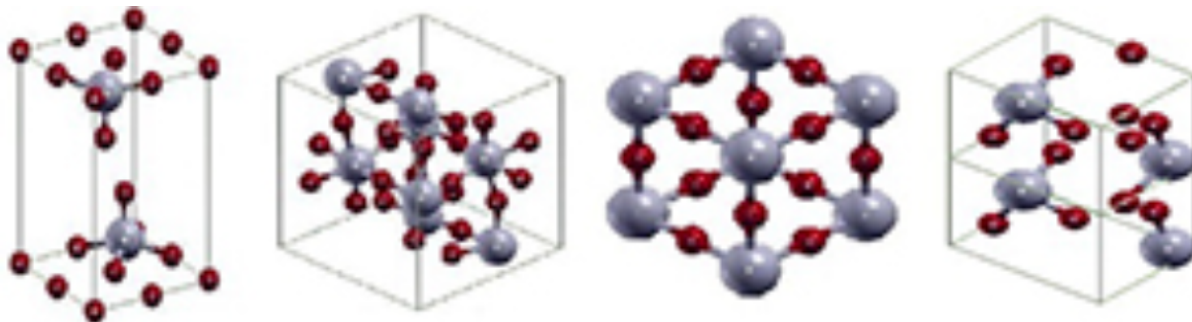


**Figure 1.** Super cells of four polymorphs.

The BS, DOS, and PDOS plots for all kinds of lattices are illustrated in Figures 2–5 with the Fermi energies indicated. Total density of states for all the electrons is depicted in Figures 2–5a. The common features of these plots show that the valance band (VB) is completely full and the Fermi level is at the position of  $E_{HUMO}$  exactly. There are three more bands deep below the VB. Hence  $WO_3$  is a semiconductor in all polymorphs.

**Table.** Lattice parameter and energetic of  $WO_3$  polymorphs.

Lattice	Lattice parameter			$E_{HUMO}$	$E_{LOMO}$	$E_{gap}$ (eV)
	a (Å)	b (Å)	c (Å)	(eV)	(eV)	type
Tetragonal	5.28	5.28	7.86	-0.97	0.25	1.22 (D)
Orthorhombic	7.86	7.57	7.81	11.82	13.20	1.38 (ID)
Monoclinic	7.30	7.53	7.68	7.60	9.60	2.03 (D)
Cubic	3.81	3.81	3.81	6.02	6.70	0.68 (ID)

Moreover, the spin polarized calculation shows that total magnetization for all of the  $WO_3$  polymorphs is zero. The results for spin up and down density of state in the monoclinic lattice (as an example) are illustrated in Figure 4a. The symmetry of these plots shows that the numbers of electrons with spin up and down are exactly the same and thereby no spin magnetization occurs.

In Figures 2–5b, density of states of VB and CB is presented. In orthorhombic and monoclinic systems there is a relatively uniform concentration of states in VB, while it is more dispersive in tetragonal and cubic systems and leads to a VB of 6.33 eV and 7.6 eV widths, respectively. Number of valance electrons can be calculated through the integral of the VB. There are 36 valance electrons in super cells with 8 atoms in them and 144 electrons in monoclinic with a 32 atom super cell. Furthermore, as indicated in PDOS plots in Figure 2–5c, the VB is made of oxygen p-orbitals and tungsten d-orbitals. Therefore, each W atom with  $[Xe]4f^{14} 5d^4 6s^2$  electronic configuration shares 4 d-electrons and each O atom with  $[He]2s^2 2p^4$  electronic configuration shares 4 p-electrons in the VB.

PDOS plots have more detailed information. Although tungsten d-orbital and oxygen p-orbital have the most prominent contribution in the VB, near edge electrons have a p-like character and localized d-electrons are about 1 eV deep inside the VB. On the other hand, CB near edge electrons is made of d-electrons dominantly. Because of these features  $WO_3$  has weaker bonding than other transition metal oxides such as  $TiO_2$  and  $ZnO$ , which leads to structural diversity in it.

Although the size of the band gap can be calculated via both DOS and BS plots, DOS has not yielded the type of it. Figures 2–5d show the band structures for all cases. The smallest band gap, as indicated in the Table, belongs to the cubic structure with an indirect gap of 0.67 eV in direction  $R \rightarrow \Gamma$ , while the largest one is for the monoclinic lattice with a direct gap of 2.03 eV at  $\Gamma$  point. This is in accordance with experimental measurements that show an energy gap of 2.7–3 eV for monoclinic  $WO_3$  [6–8]. It should be noted that DFT underestimates the band gap. Indeed, this band gap corresponds to the visible range of light. Specifically, because the most stable structure of  $WO_3$  in room temperature is monoclinic, it is an appropriate material for implementing in optical devices. The tetragonal structure of  $WO_3$  has also displayed a direct band gap of 1.22 eV at  $\Gamma$  point that is not in the visible range. However,  $WO_3$  in the orthorhombic structure is a semiconductor with an indirect gap of 1.4 eV ( $E \rightarrow \Gamma$ ).

#### 4. Conclusion

It has been found that tungsten trioxide has a temperature dependent structure, with four polymorphs. We have done an ab initio calculation in the DFT framework to explore the electronic properties of these polymorphs. Our results show that  $WO_3$  is a nonmagnetic semiconductor in all four crystal lattices of monoclinic, orthorhombic, tetragonal, and cubic. The electronic d-orbitals are located deep inside the VB, while p-orbitals determine the characteristic of VB edge electrons, which contribute in electronic transport. Moreover,  $WO_3$  has an indirect

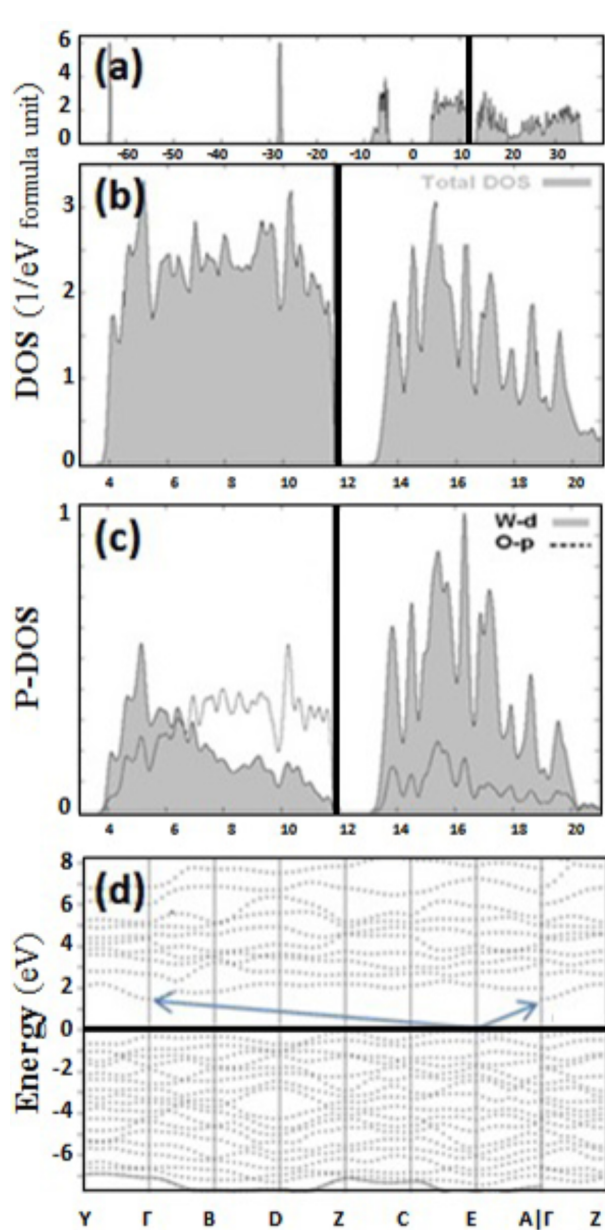


**Figure 2.** Total DOS (a), VB and CB DOS (b), PDOS (c), and BS (d) for orthorhombic  $WO_3$ .

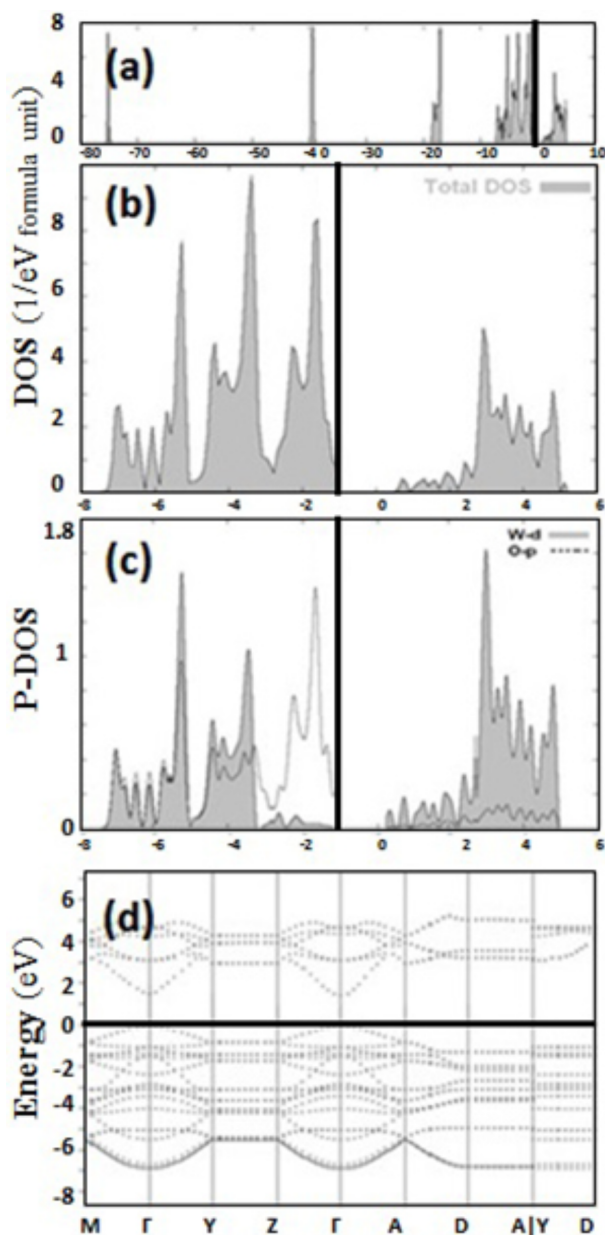


**Figure 3.** Total DOS (a), VB and CB DOS (b), PDOS (c), and BS (d) for tetragonal  $WO_3$ .

band gap of 0.67 eV and 1.4 eV in cubic and orthorhombic lattices, respectively, and a direct band gap of 2.03 eV and 1.22 eV in monoclinic and tetragonal structures, respectively.

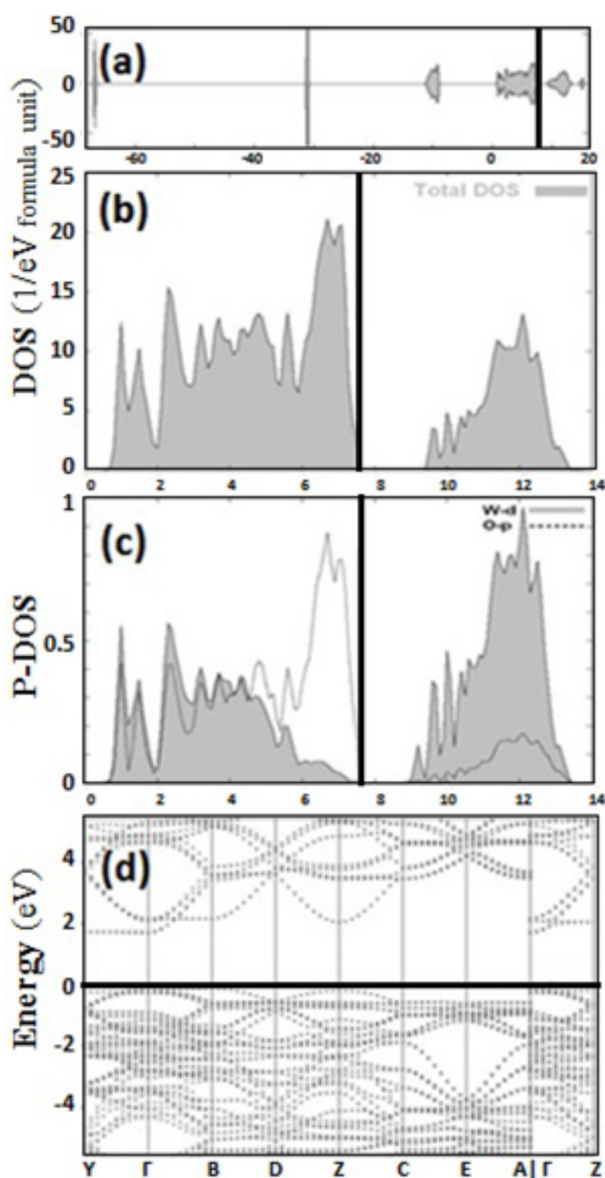


**Figure 4.** Total DOS (a), VB and CB DOS (b), PDOS (c), and BS (d) for cubic  $WO_3$ .

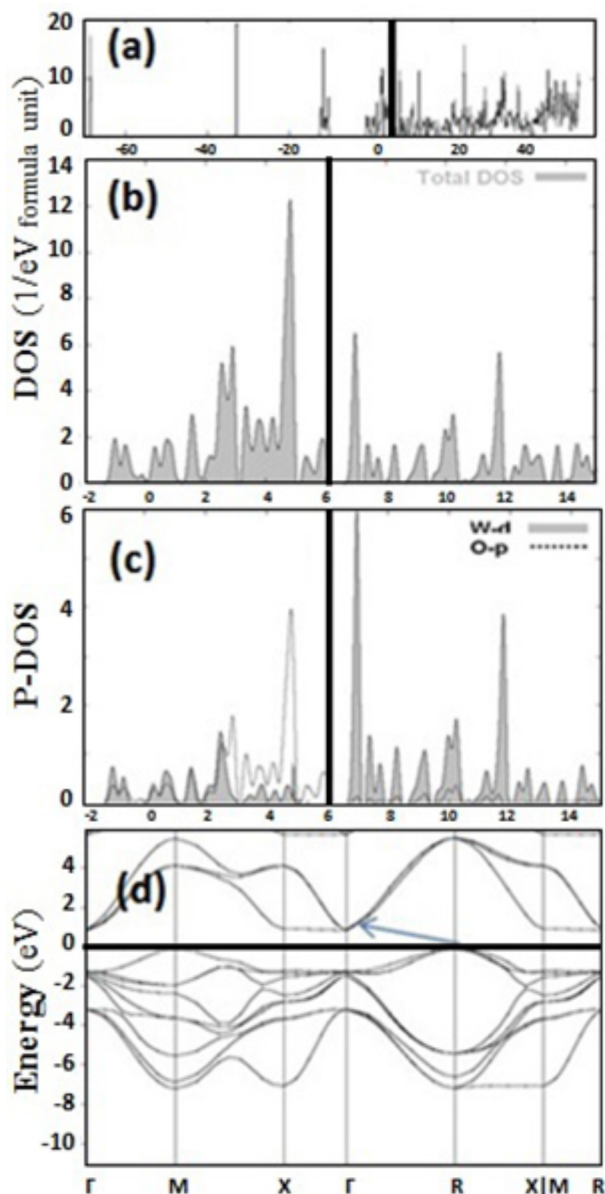


**Figure 5.** Total DOS (a), VB and CB DOS (b), PDOS (c), and BS (d) for monoclinic  $WO_3$ .

### References

- [1] Lee, W. J.; Fang, Y. K.; Ho, J. J.; Hsieh, W. T.; Ting, S. F.; Huang, D.; Ho, F. *J. Electron. Matter.* **2000**, *29*, 183-187.
- [2] Reich, S.; Leitus, G.; Tssaba, Y.; Levi, Y.; Sharoni, A.; Millo, O. *J. Supercond.* **2000**, *13*, 855-861.
- [3] Yamazoe, N.; Sakai, G.; Shimano, K. *Catalysis Surveys from Asia* **2003**, *7*, 63-75.
- [4] Liang, L.; Zhang, J.; Zhou, Y.; Xie, J.; Zhang, X.; Guan, M. *Sci. Rep.* **2013**, *3*, 1936.
- [5] Xue, X. Y.; He, B.; Yuan, S.; Xing, L. L.; Chen, Z. H.; Ma, C. H. *Nanotechnology* **2011**, *22*, 395702.
- [6] Bocharov, D.; Kuzmin, A.; Purans, J.; Zhukovskii, Y. In *Conference Proceedings: 8th Intl Symp on Gas Flow and Chemical Lasers*, International Society for Optics and Photonics, 2008, pp. 71420-71429.

- [7] Hu, M.; Jie, Z.; Wang, W. D.; Qin, Y. X. *Chin. Phys. B.* **2011**, *20*, 082101.
- [8] Bullett, D. *J. Phys. C: Solid State Physics* **1983**, *16*, 2197-2207.
- [9] Loopstra, B.; Rietveld, H. *Acta Cryst. B* **1969**, *25*, 1420-1421.
- [10] Giannozzi, P.; Baroni, S.; Bonini, N.; Calandra, M.; Car, R.; Cavazzoni, C. *J. Phys. Condens. Matter* **2009**, *21*, 395502-395521.
- [11] Kohn, W.; Becke, A. D.; Parr, R. G. *J. Phys. Chem.* **1996**, *100*, 12974-12980.
- [12] Ernzerhof, M., Scuseria, G. E. *J. Chem. Phys.* **1999**, *110*, 5029-5036.
- [13] Perdew, J. P., Burke, M., Ernzerhof, M. *Phys. Rev. Lett.* **1996**, *77*, 3865-3868.
- [14] Monkhorst, H. J., Pack, J. D. *Phys. Rev. B* **1976**, *13*, 5188-5192.